

## ESS DTL STATUS: REDESIGN AND OPTIMIZATIONS

R. De Prisco\*, ESS, Lund, Sweden and Lund University, Lund, Sweden  
 M. Comunian, F. Grespan, A. Pisent, INFN/LNL, Legnaro, Italy  
 M. Eshraqi, ESS, Lund, Sweden,  
 A. Karlsson, Lund University, Lund, Sweden

### Abstract

The European Spallation Source (ESS) uses a linear accelerator to deliver the high intensity proton beam to the target station. The average beam power is 5 MW with a peak beam power at target of 125 MW. In 2013 the ESS linac was costed and to meet the budget some modifications were introduced: the final energy was decreased from 2.5 GeV to 2.0 GeV and the beam current was increased from 50 mA to 62.5 mA to keep the same beam power [1]. As a consequence the ESS Drift Tube Linac, DTL, has been re-designed to match the new requirements. This paper presents the main Radio Frequency (RF) and beam dynamics choices for the ESS DTL.

### INTRODUCTION

In the actual design the DTL accelerates a proton beam of 62.5 mA from 3.62 MeV to 89.68 MeV at 352.21 MHz. The pulses are 2.86 ms long with a duty cycles of 4%. Permanent Magnet Quadrupoles (PMQs) are used as focusing elements in a FODO lattice.

### RF DESIGN

The cell geometry is designed to meet many requirements: sufficient space to accommodate PMQs, mitigation of the risk of breakdown and multipacting in particular at the low energy part. The maximum tank length is equal to 8 m to preserve the RF voltage stability. The mechanical modules, or sub-tanks, have a maximum length of 2 m. The geometric parameters of the ESS DTL are shown in the Fig. 1 and summarized in Table 1. The actual design consists of 5 tanks (4 in the previous version [4]) with flat accelerating field even in the first tank (ramped in the previous version).

Table 1: Geometric Tank Properties of the ESS DTL

Tank	1	2	3	4	5
Modules [#]	4	4	4	4	4
Cells [#]	61	34	29	26	23
$L_T$ [mm]	7618	7101	7583	7847	7687
$R_b$ [mm]	10	11	11	12	12
$R_o$ [mm]	8	8	8	8	8
$R_c$ [mm]	5	5	5	5	5
$R_i$ [mm]	3	3	3	3	3
F [mm]	3	3	3	3	3
d [mm]	90	90	90	90	90
D [mm]	520	520	520	520	520

\* renato.deprisco@esss.se

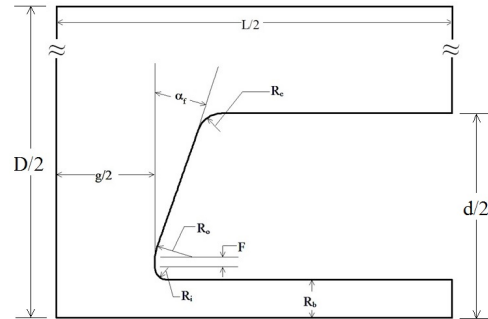


Figure 1: Representative longitudinal cross section of half unit cell geometry: Tank Diameter,  $D$ ; cell Length,  $L$ ; gap length,  $g$ ; drift tube diameter,  $d$ ; bore Radius,  $R_b$ ; Flat length,  $F$ ; inner nose Radius,  $R_i$ ; outer nose Radius,  $R_o$ ; face angle,  $\alpha_f$ .

The synchronous phase, shown in the Fig. 2, is ramped in the first tank from  $-35^\circ$  to  $-25.5^\circ$ ; equal to  $-25.5^\circ$  elsewhere. In order to compensate the effect of the missing gap between two consecutive tanks the synchronous phase gradually is decreased to  $-35^\circ$  in the two cells before and after each intertank; it is decreased to  $-43.5^\circ$  in the last three cells of the fifth tank in order to match the beam to the spoke cavities.

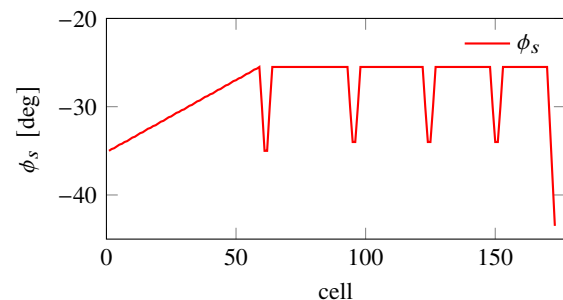


Figure 2: Synchronous phase.

The average electric accelerating field,  $E_0$ , shown in Fig. 3, is constant in each tank and optimized [2] in order to reach the maximum energy gain per tank. The available RF power per tank is equal to 2.2 MW, by including a factor of 1.25 over the MDTfish power computation.

The peak electric field, shown in the Fig. 3, is ramped from 1.20 Kilp. to 1.55 Kilp. in the first 20 cells of the first tank in order to reduce the breakdown probability; then it is equal to 1.55 Kilp. in the last cells of the first tank; lower than 1.55 Kilp. elsewhere.

Content from this work may be used under the terms of the CC BY 3.0 licence (© 2014). Any distribution of this work must maintain attribution to the author(s), title of the work, publisher, and DOI.

Table 2: Accelerating Field Integral,  $E_0$ , Maximum Electric Field,  $E_{MAX}$ , Output Energy,  $E_{OUT}$ , and Dissipated Power,  $P_{TOT}$ , in each Tank

Tank	1	2	3	4	5
$E_0$ [MV/m]	3.00	3.16	3.07	3.04	3.13
$E_{MAX}$ [Kilp.]	1.55	1.55	1.55	1.55	1.55
$E_{OUT}$ [MeV]	21.29	39.11	56.81	73.83	89.68
$P_{TOT}$ [kW]	2192	2191	2196	2189	2195

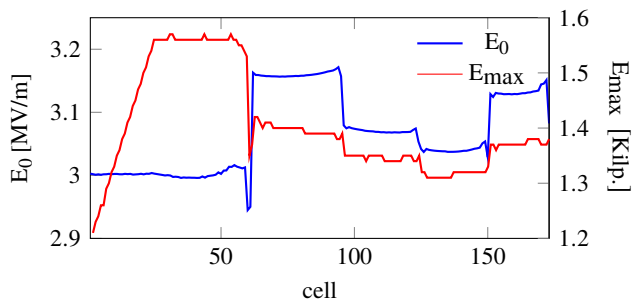


Figure 3: Accelerating field integral and maximum cell electric field (1 Kilp. = 18.4 MV/m at 352.21MHz).

The main RF parameters are summarized in the Table 2. Every cell is designed by tuning of the cell length, gap and face angles in order to meet the requirements, to be resonant at the design frequency and to maximize the effective shunt impedance, shown in Fig. 4.

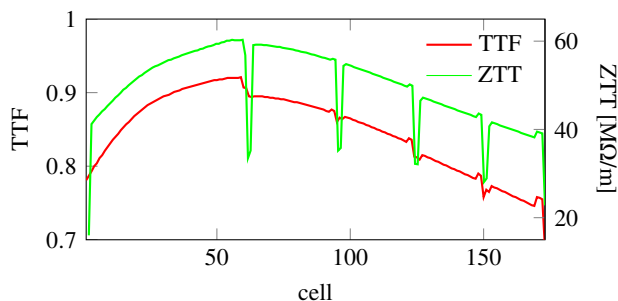


Figure 4: Transit Time Factor, TTF, and effective shunt impedance, ZTT.

### Permanent Magnet Quadrupole

The transverse focusing is performed by 16-segmented Halbach PMQs of samarium cobalt in vacuum and settled in a FODO lattice [4]. Each segment has a X-section of 4 mm×14 mm; PMQ outer diameter is equal to 60 mm while the inner radius is equal to the bore radius plus 1 mm. There are 31 PMQs of 50 mm length in the first tank and 58 of 80 mm in the rest. The PMQ maximum gradient is equal to 61.46 T/m as shown in the in the Fig. 5.

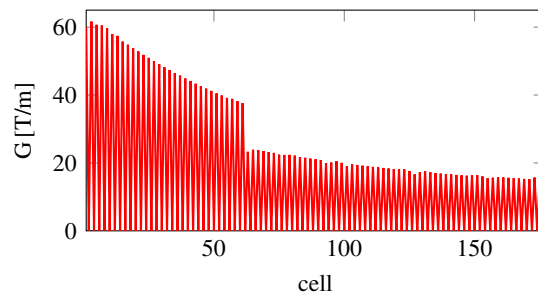


Figure 5: PMQ gradient.

### Power Coupler

The power is delivered to each tank by two iris power couplers with 1.1 MW peak power each. They are located at 1/3 and 2/3 of the tank's longitudinal length.

### Tuning Range

Movable tuners, at least two for each tank, will compensate the thermal expansion causing dynamic frequency changes: thermo-mechanical simulations are running to define their number.

The evaluation of static frequency error, due to machining error, is done by applying realistic tolerances on the geometrical parameters defined in the Table 1. Static tuners compensate the frequency shift due to construction errors: they have a diameter of 90 mm, are distributed uniformly every 30 cm along the tank and are located at 45° with respect to the stem axis in order to avoid a frequency shift of the Post Couplers, PC, 0-mode by tuner penetration. The tuner sensitivity is 6.02(kHz/mm)×m, linear around 30 mm of penetration.

### Stabilization

Assuming the worst case perturbations of the end cells in the first tank, which is the most sensitive, and that the PCs are inserted with their optimum length the stabilization depends essentially on the distance between two consecutive PCs [5]. This length in the case of the ESS DTL is around 33 cm [2] to keep  $E_0$  within 1% of its nominal value: the number of PCs per tank is summarized in the Table 3.

Table 3: Number of Post Couplers per Tank

Tank	1	2	3	4	5
PCs [#]	23	22	28	25	22

### Compensation of Stem and PC Effect

The frequency perturbation of the stems and the PCs is compensated locally by face angles [2].

## BEAM PHYSICS

The Beam Dynamics (BD) performance of the ESS DTL is evaluated by assuming a transverse RMS emittance equal to 0.28 π.mm.mrad, longitudinal RMS emittance equal to

0.1436  $\pi$ .deg.MeV, matched twiss parameters at the DTL input and uniform particle distribution.

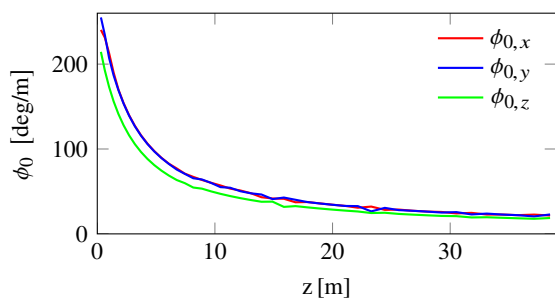


Figure 6: 0-current phase advance in x (red), y (blue) and z (green).

The transverse and the longitudinal phase advance, shown in the Fig. 6, have been optimized in all five tanks in order to have a smooth transition minimizing the emittance growth and avoiding the resonances. The external focusing strength is limited in order to have the zero-current phase advance less than  $90^\circ$  per period. The tune depression (ratio of the phase advance with and without space charge), shown in the in the Fig. 7, is kept above 0.4 [3].

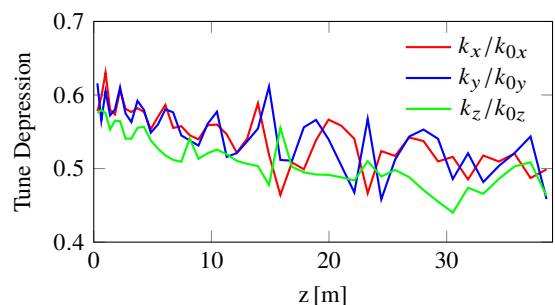


Figure 7: Tune depression in x (red), y (blue) and z (green).

A measure of the design solidity is given by the ratio of the bore radius over the RMS beam: in the transverse plane it is always greater than 4.

The emittance growth along the DTL is equal to 2% both in transverse and longitudinal plane (Fig. 8).

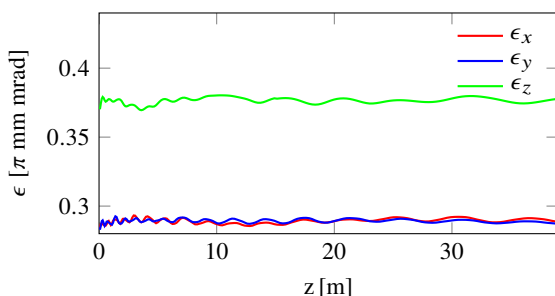


Figure 8: Emittance in x (red), y (blue) and z (green).

The transverse acceptance is equal to  $14 \pi$ .mm.mrad and the longitudinal is equal to  $12 \pi$ .deg.MeV.

## ERROR STUDY

To evaluate the robustness of the ESS DTL a statistical error study has been performed by applying errors (Table 4) on the PMQ alignment ( $dx$ ,  $dy$ ), rotation ( $d\phi_x$ ,  $d\phi_y$  and  $d\phi_z$ ) and gradient ( $\Delta G$ ), on field,  $\Delta E_0$ , and phase,  $\Delta\phi_s$ , of each cell, on klystron field,  $\Delta E_k$ , and phase,  $\Delta\phi_k$ , and their jitters ( $\Delta E_{k,d}$  and  $\Delta\phi_{k,d}$ ). In order to simulate a realistic input beam distribution a gaussian beam of  $10^6$  macro particles, truncated at  $4\sigma$ , was transported from the radio frequency quadrupole to the DTL by applying realistic tolerances for all the inter-structures. Three steerers per tank per plane (X and Y) with maximum strength of 0.8 mT.m are used to correct the beam centroid.

Table 4: Range of Errors

Parameter	Tolerance
$dx$ , $dy$ [mm]	0.1
$d\phi_x$ , $d\phi_y$ [deg]	0.5
$d\phi_z$ [deg]	0.2
$\Delta G$ [%]	0.5
$\Delta E_0$ [%]	1
$\Delta\phi_s$ [deg]	0.5
$\Delta E_k$ , $\Delta E_{k,d}$ [%]	1, 0.1
$\Delta\phi_k$ , $\Delta\phi_{k,d}$ [deg]	1, 0.1

The study, based on over 1000 runs, shows that the average losses are equal to 0.14 W and that the difference between the emittance growth with and without errors is equal to 6% in the transverse and to 7% in the longitudinal plane.

To define the manufacturing tolerances of the machine components, the optimum steerer number and strength a campaign of statistical error studies is ongoing.

## CONCLUSION

The ESS DTL has been redesigned to match the new requirements. Many RF and BD optimizations were done to reach the maximum energy gain and to reduce losses and emittance growth. The error study shows that the DTL is robust and well integrated in the ESS linear accelerator.

## REFERENCES

- [1] M. Eshraqi et al., "THE ESS LINAC," IPAC'14, Dresden, June 2014, *These Proceedings*.
- [2] R. De Prisco et al., "ESS DTL RF Modelization: Field Tuning and Stabilization," IPAC'13, Shanghai, May 2013, TH-PWO070, p. 3918.
- [3] J-M. Lagniel., "Halos and Chaos in Space-Charge Dominated Beams," EPAC'96, Barcelona, June 1996, WEY01A, p. 163.
- [4] M. Comunian et al., "Progress on DTL Design for ESS," IPAC'13, Shanghai, May 2013, THPWO024, p. 3815.
- [5] F. Grespan, "Equivalent Circuit for Postcoupler Stabilization in a Drift Tune LINAC," Phys. Rev. ST Accel. Beams, 15(1), 010101, January 2012, DOI:10.1103/PhysRevSTAB.15.010101.